International Journal of the Physical Sciences Vol. 6(21), pp. 4910-4923, 30 September, 2011
Available online at http://www.academicjournals.org/IJPS
DOI: 10.5897/IJPS11.295
ISSN 1992 - 1950 ©2011 Academic Journals

Full Length Research Paper

Convection from a semi-finite plate in a fluid saturated porous medium with cross-diffusion and radiative heat transfer

F. G. Awad, P. Sibanda*, M. Narayana and S. S. Motsa

School of Mathematical Sciences, University of KwaZulu-Natal, Private Bag X01 Scottsville 3209, Pietermaritzburg, South Africa.

Accepted 5 July, 2011

The heat and mass transfer characteristics in mixed convection along a semi-infinite plate in a fluid saturated porous medium with radiative heat transfer has been investigated. Diffusion-thermo and thermo-diffusion effects are assumed to be significant. Using a similarity transformation, the governing steady boundary layer equations for the momentum, heat and mass transfer were reduced to a set of ordinary differential equations and then solved using a recent novel linearization method and the Keller-box method. The results were further confirmed by using the Matlab bvp4c numerical routine. The effects of the Dufour and Soret parameters on the local skin friction and the local heat and mass transfer rates are investigated. Numerical results for the velocity and the temperature profiles are also presented.

Key words: Vertical flat plate, porous medium, cross diffusion, radiation, successive linearization method.

INTRODUCTION

Free convention flow due to thermal and mass diffusion has received widespread attention due to the importance of heat and mass transfer in engineering processes such as in petroleum and geothermal processes, drying, moisture migration in fibrous insulation, nuclear waste disposal and in the control of pollutant spread in ground water. Double diffusive convection driven by buoyancy due to temperature and concentration gradients has been studied by many researchers, among them Erickson et al. (1996) and Fox et al. (1968) who studied the effects of suction and injection on the problem of heat and mass transfer in the laminar boundary layer flow of moving flat surface with constant surface velocity and temperature. Gupta and Gupta (1977) studied heat and mass transfer in the boundary layer over a stretching sheet with suction or blowing. Bejan and Khair (1985) investigated the free convection boundary layer flow in a porous medium due to combined heat and mass transfer.

*Corresponding author. E-mail: sibandap@ukzn.ac.za.

Heat and mass diffusing simultaneously give rise to the cross-diffusion effect. Weaver and Viskanta (1991) have pointed out that when the differences in the temperature and the concentration are large or when the difference in the molecular mass of two elements in a binary mixture is large, the coupled interaction is significant. The mass transfer caused by the temperature gradient is referred to as the Soret effect, while the heat transfer caused by the concentration gradient is called the Dufour effect (Mortimer and Eyringt, 1980; Tsai and Huang, 2009; Awad et al., 2010). Eckert and Drake (1972) presented several examples of the Dufour effect and reported that the Dufour effect was, in many instances, of sufficiently high order of magnitude such that it cannot be ignored. Investigations by Atimtay and Gill (1985), Rosner (1980) and Yu et al. (2007) have also shown that Soret mass flux and Dufour energy flux have appreciable and at times significant effect on heat and mass transfer rates. Atimay and Gill (1985) showed that an error as large as 30% in the wall mass flux could be expected if the Soret effect is neglected.

Anghel et al. (2000) investigated the Dufour and Soret

effects in free convection on a boundary layer formed by a vertical surface embedded in a porous medium. A discussion of the effects of coupled cross-diffusion in a system with temperature and concentration gradients is given (Malashetty and Gaikad, 2002). Alam et al. (2006) and Postelnicu (2004) studied the influence of a magnetic field on heat and mass transfer by natural convection from vertical surfaces in porous media in the presence of Soret and Dufour effects.

Thermal diffusion and diffusion thermo effects in boundary layer due to a vertical flat plate were studied by Abreu et al. (2006). Soret and Dufour effects have been presented for the steady MHD free convection flow past a semi-infinite moving vertical plate in a porous medium with viscous dissipation (Reddy and Reddy, 2010). They used a fourth order Runge-Kutta method with a shooting technique to solve the flow equations. The effect of suction/injection on thermophoretic particle deposition in free convection on a vertical plate embedded in a fluid saturated non-Darcy porous medium was studied by Partha (2009).

Cheng (2009) studied the Dufour and Soret effects on the steady boundary layer flow due to natural convection heat and mass transfer over a downward-pointing vertical cone embedded in a porous medium saturated with Newtonian fluids with constant wall temperature and concentration. Mahdy (2010) numerically studied the mixed convection from a vertical isothermal surface embedded in a porous medium saturated with the Ostwald de-Waele type of non-Newtonian fluid under the influence of Soret and Dufour effects.

For a vertical wavy surface in a Newtonian fluid saturated Darcy porous medium, Narayana and Sibanda (2010) investigated free convection of heat and mass transfer in the presence of cross diffusion numerically. The recent study by Awad et al. (2010) investigated the stability of double-diffusive convection of a Maxwell fluid in a high porosity porous medium taking cross-diffusion effects into account. The criterion for the onset of stationary and oscillatory convection was derived analytically in terms of the critical Darcy-Rayleigh number. In a recent study, Shateyi et al. (2010) investigated the effects of thermal radiation, Hall currents, Soret and Dufour on MHD flow by mixed convection over a vertical surface in porous media. They showed among other results that the temperature increased with the Dufour parameter but that the concentration decreased as the Dufour number increased.

Thermal radiation effects on heat and mass transfer over unsteady stretching surface was recently investigated by Shateyi and Motsa (2009) where a Chebyshev pseudo spectral collocation method was used to solve the governing equations. Studies by Hossain and Takhar (1996), Rapits and Perdikis (1998), Makinde and Ogulu (2008) and El-Aziz (2009) are earlier investigations of the thermal radiation effects. Rapits (1998) studied the flow of a visco-elastic fluid and micropolar fluid past a stretching sheet in the presence of thermal radiation.

In this work linearization technique and the Keller-box implicit method were used to find solutions of the coupled nonlinear equations that govern free convection from a semi-finite plate saturated in a porous medium in the presence of Dufour energy flux and Soret mass flux. The study extends the earlier work by Parand et al. (2010) to include Dufour and Soret effects. The paper further extends the study by Alam et al. (2006) to include radiative heat transfer. The study differs from Shateyi et al. (2010) in that it includes neither the effects of applied magnetic field nor Hall effects. We show by comparison with numerical results and previous studies that the linearization method is accurate and converges rapidly to the true solution.

MATHEMATICAL FORMULATION

Consider the steady two-dimensional flow along a vertical flat plate embedded in a fluid-saturated porous medium. The *y*-axis is measured along the flat surface and *x*-axis normal to it. Assuming the validity of the Boussinesq and boundary layer approximations, the governing equations are shown as follows:

$$\frac{\partial u}{\partial x} + \frac{\partial v}{\partial y} = 0 \tag{1}$$

$$u\frac{\partial u}{\partial x} + v\frac{\partial u}{\partial y} = \upsilon\frac{\partial^2 u}{\partial y^2} - \frac{\nu}{K}u + \rho g\beta_T(T - T_\infty) + \rho g\beta_C(C - C_\infty), \tag{2}$$

$$u\frac{\partial T}{\partial x} + v\frac{\partial T}{\partial y} = \frac{k}{\rho c_p}\frac{\partial^2 T}{\partial y^2} - \frac{1}{\rho c_p}\frac{\partial q_r}{\partial y} + \frac{D_1}{c_s c_p}\frac{\partial^2 C}{\partial y^2} \tag{3}$$

$$u\frac{\partial C}{\partial x} + v\frac{\partial C}{\partial y} = D^*\frac{\partial^2 C}{\partial y^2} + \frac{D_2}{c_s c_p}\frac{\partial^2 T}{\partial y^2}, \tag{4}$$

subject to the boundary conditions

$$u(0) = v(0) = 0,\ T(0) = T_w,\ C(0) = C_w, \tag{5}$$

$$u(\infty) = U_\infty,\ \ T(\infty) = T_\infty,\ C(\infty) = C_\infty, \tag{6}$$

where u and v are the velocity components along the x- and y-axes, respectively, υ is the kinematic viscosity, ρ is the fluid density, T and C are the fluid temperature and concentration across the boundary layer, c_p is the fluid specific heat, k and D^* are the thermal conductivity and solutal diffusivity, respectively. D_1 and D_2 are parameters quantifying the contribution to heat flux due to the concentration gradient and mass flux due to temperature gradient, respectively, q_r is the radiative heat flux, β_T is the coefficient of thermal expansion, β_C is the volumetric coefficient of expansion with concentration, T_w is a constant temperature of the wall, T_∞ is the ambient fluid temperature, $T_\infty > T_w$ and U_∞ is a constant free

stream velocity. It is assumed that the viscous dissipation is neglected. Using the Rosseland approximation, the radiative heat flux is given as the following:

$$q_r = \frac{4\sigma^*}{3k^*}\frac{\partial T^4}{\partial y} \tag{7}$$

where σ^* and k^* are the Stefan-Boltzmann constant and the mean absorption coefficient, respectively. We assume that the term T^4 may be expressed as a linear function,

$$T^4 \cong 4T_\infty^3 T - 3T_\infty^4 \tag{8}$$

Using Equations 7 and 8 in Equation 3, yields

$$u\frac{\partial T}{\partial x} + v\frac{\partial T}{\partial y} = \frac{\alpha}{k_0}\frac{\partial^2 T}{\partial y^2} + \frac{D_1}{c_s c_p}\frac{\partial^2 C}{\partial y^2}, \tag{9}$$

where $\alpha = k/\rho c_p$, is the thermal diffusivity and $k_0 = 3N_R/(3N_R+4)$ and $N_R = kk^*/4\sigma^* T_\infty^3$. The effect of radiation is to enhance the thermal diffusivity.

We introduce a similarity variable η, dimensionless stream function f, temperature θ and the solute concentration Φ where

$$\eta = y\sqrt{\frac{U_\infty}{\nu x}},\ \psi = \sqrt{\nu U_\infty x}f(\eta),\ \theta(\eta) = \frac{T - T_\infty}{T_w - T_\infty},\ \ \phi(\eta) = \frac{C - C_\infty}{C_w - C_\infty}. \tag{10}$$

The stream function $\psi(x, y)$ is defined by

$$u = \frac{\partial \psi}{\partial y},\ v = -\frac{\partial \psi}{\partial x},$$

so that the continuity Equation 1 is satisfied identically. The velocity components are given by

$$u = U_\infty f',\quad v = \frac{1}{2}\sqrt{\frac{U_\infty \nu}{x}}(\eta f' - f), \tag{11}$$

where the prime denotes differentiation with respect to η. Substituting Equation10 into Equations 1 to 4, we get the coupled nonlinear system as the following;

$$f''' + \frac{1}{2}ff'' + g_s\theta + g_c\phi - \frac{1}{\mathrm{Re}_D}f' = 0, \tag{12}$$

$$\theta'' + D_f\phi'' + \frac{1}{2}k_0 \Pr f\theta' = 0, \tag{13}$$

$$\phi'' + S_r\theta'' + \frac{1}{2}Scf\phi' = 0. \tag{14}$$

Equations 12 and 13 have to be solved subject to the boundary conditions

$$\begin{aligned} &f = 0,\ f' = 0,\ \theta = \phi = 1 \text{ at } \eta = 0,\\ &f' = 1,\ \theta = 0 \text{ and } \phi = 0 \text{ as } \eta \to \infty. \end{aligned} \tag{15}$$

In Equations 12 to 14 Re_D is the Darcy-Reynolds number, *Pr* is the Prandtl number, *Sc* is the Schmidt number, D_f is the Dufour number, S_r is the Soret number, g_s is the temperature buoyancy parameter and g_c is the mass buoyancy parameter. These quantities are defined by the following;

$$Da = \frac{K}{x^2},\ \mathrm{Re}_D = \frac{1}{Da\ \mathrm{Re}_x},\ \mathrm{Re}_x = \frac{U_\infty x}{\nu},\ \Pr = \frac{\nu}{\alpha},\ Sc = \frac{\nu}{D^*},$$

$$D_f = \frac{D_1 k_0}{\alpha c_s c_p}\frac{C_\infty - C_w}{T_\infty - T_w},\ S_r = \frac{D_2}{\alpha c_s c_p}\frac{T_\infty - T_w}{C_\infty - C_w},\ g_c = \frac{Gr_m}{\mathrm{Re}_x^2},$$

$$Gr_m = \frac{\rho g \beta_C (C_\infty - C_w)x^3}{\nu^2},\ Gr_x = \frac{\rho g \beta_T (T_\infty - T_w)x^3}{\nu^2},\ g_s = \frac{Gr_x}{\mathrm{Re}_x^2},$$

where Gr_x is the local temperature Grashof number, Gr_m is the mass Grashof number, Re_x is the local Reynolds number and Da is the Darcy number.

In this study only a local similarity solution is obtained. Full similarity solutions with all the physical parameters independent of x are possible, for example, when the boundary temperature and concentration vary linearly with x, that is, when

$$T = T_\infty + Ax \quad \text{and} \quad C = C_\infty + Bx \quad \text{at} \quad y = 0,$$

where A and B are constants. In all other cases only local similarity solutions are obtained.

The parameters of engineering interest in any heat and mass problem are the local Nusselt number Nu_x and Sherwood number Sh_x. These parameters characterize the surface heat and mass

transfer rates, respectively, and is defined by the equation that follows;

$$Nu_x = -\mathrm{Re}_x^{1/2}\,\theta'(0) \quad \text{and} \quad Sh_x = -\mathrm{Re}_x^{1/2}\,\phi'(0). \tag{16}$$

METHOD OF SOLUTION

Equations 12 to 14 were solved using a novel successive linearization method (Awad et al., 2011; Motsa et al., 2011). This method assumes that the independent variables can be expanded in the following form;

$$f(\eta) = f_i(\eta) + \sum_{n=0}^{i-1} f_n(\eta),$$

$$\theta(\eta) = \theta_i + \sum_{n=0}^{i-1} \theta_n(\eta),$$

$$\phi(\eta) = \phi_i(\eta) + \sum_{n=0}^{i-1} \phi_n(\eta)$$

where f_i, θ_i and ϕ_i $(i = 1,2,3,\ldots)$ satisfy the conditions

$$\lim_{i\to\infty} f_i(\eta) = \lim_{i\to\infty} \theta_i = \lim_{i\to\infty} \phi_i(\eta) = 0.$$

The functions $f(\eta)$, $\theta(\eta)$ and $\phi(\eta)$ $(n \geq 1)$ are approximations which are obtained by recursively solving the linear parts of the equation system that results from substituting these expansions in Equations 12 to 14. Using the earlier assumptions, nonlinear terms in f_i, θ_i, ϕ_i and their corresponding derivatives are considered to be very small and therefore neglected. Starting from the initial guesses $f_0(\eta)$, $\theta_0(\eta)$, $\phi_0(\eta)$, which are chosen to satisfy boundary conditions of Equation 14, the subsequent solutions for $n \geq 1$ are obtained by successively solving the linearized form of the equations.

The linearized equations to be solved are shown as;

$$f_i''' + a_{1,i-1} f_i'' - \frac{1}{\mathrm{Re}_D} f_i' + a_{2,i-1} f_i + g_s \theta_i + g_c \phi_i = r_{1,i-1}, \tag{17}$$

$$\theta_i'' + b_{1,i-1}\theta_i' + b_{2,i-1} f_i + D_f \phi_{ii}'' = r_{2,i-1}, \tag{18}$$

$$\phi_i'' + c_{1,i-1}\phi_i' + c_{2,i-1} f_i + Sr\,\theta'' = r_{3,i-1}, \tag{19}$$

subject to the boundary conditions

$$f_i(i) = f_i'(0) = f'(\infty) = 0,\ \theta_i(0) = \theta_i(\infty) = \phi_i(0) = \phi_i(\infty) = 0, \tag{20}$$

where the coefficient parameters are defined as the following;

$$a_{1,i-1} = \frac{1}{2}\sum_{n=0}^{i-1} f_n, \quad a_{2,i-1} = \frac{1}{2}\sum_{n=0}^{i-1} f_n'', \tag{21}$$

$$b_{1,i-1} = \frac{\mathrm{Pr}\ k_0}{2}\sum_{n=0}^{i-1} f_n, \quad b_{2,i-1} = \frac{\mathrm{Pr}\ k_0}{2}\sum_{n=0}^{i-1} \theta_n', \tag{22}$$

$$c_{1,i-1} = \frac{Sc}{2}\sum_{n=0}^{i-1} f_n, \quad c_{2,i-1} = \frac{Sc}{2}\sum_{n=0}^{i-1} \phi_n', \tag{23}$$

$$r_{1,i-1} = -\left[\frac{1}{2}\sum_{n=0}^{i-1} f_n''' + \frac{1}{2}\sum_{n=0}^{i-1} f_n \sum f_n'' - \frac{1}{\mathrm{Re}_D}\sum_{n=0}^{i-1} f_n' + g_s\sum_{n=0}^{i-1}\theta_n + g_c\sum_{n=0}^{i-1}\phi_n\right], \tag{24}$$

$$r_{2,i-1} = -\left[\sum_{n=0}^{i-1}\theta_n'' + D_f\sum_{n=0}^{i-1}\phi_n'' + \frac{\mathrm{Pr}\ k_0}{2}\sum_{n=0}^{i-1} f_n\sum_{n=0}^{i-1}\theta_n'\right], \tag{25}$$

$$r_{3,i-1} = -\left[\sum_{n=0}^{i-1}\phi_n'' + Sr\sum_{n=0}^{i-1}\theta_n'' + \frac{Sc}{2}\sum_{n=0}^{i-1} f_n\sum_{n=0}^{i-1}\phi_n'\right]. \tag{26}$$

The functions f_i, θ_i and ϕ_i $(i \geq 1)$ are obtained by iteratively solving Equations 17 to 19. The approximate solutions for $f(\eta)$, $\theta(\eta)$ and $\phi(\eta)$ are then obtained as the following;

$$f(\eta) \approx \sum_{m=0}^{M} f_m(\eta), \tag{27}$$

$$\theta(\eta) = \sum_{m=0}^{M} \theta_m(\eta), \tag{28}$$

$$\phi(\eta) = \sum_{m=0}^{M} \phi_m(\eta), \tag{29}$$

where *M* is the order of the SLM approximation. Equations 17 to 19 were solved using the Chebyshev spectral collocation method where the unknown functions are approximated using Chebyshev interpolating polynomials at the Gauss-Lobatto points

$$\xi_j = \cos\frac{\pi j}{N}, \quad j = 0,1,\ldots,N, \tag{30}$$

where N is the number of collocation points. The physical region

$[0,\infty]$ is first transformed into the region $[-1,1]$ using the domain truncation technique in which the problem is solved in the interval $[0, L]$ instead of $[0,\infty]$. This leads to the following mapping;

$$\frac{\eta}{L} = \frac{\xi + 1}{2}, \quad -1 \le \xi \le 1, \tag{31}$$

$$f_i(\xi) \approx \sum_{k=0}^{N} f_i(\xi_k) T_k(\xi_j), \ \theta_i(\xi) \approx \sum_{k=0}^{N} \theta_i(\xi_k) T_k(\xi_j), \phi_i \approx \sum \phi_i(\xi_k) T_k(\xi_j), \quad j = 0,1,\ldots,N \tag{32}$$

where T_k is the k^{th} Chebyshev polynomial defined as; $T_k = \cos[k\cos^{-1}(\xi)]$. (33)

The derivatives at the collocation points are represented as;

$$\frac{d^s f_i}{d\eta^s} = \sum_{k=0}^{N} \mathrm{D}_{kj}^s f_i(\xi_k), \frac{d^s \theta_i}{d\eta^s} = \sum_{k=0}^{N} \mathrm{D}_{kj}^s \theta_i(\xi_k), \frac{d^s \phi_i}{d\eta^s} = \sum_{k=0}^{N} \mathrm{D}_{kj}^s \phi_i(\xi_k), \ j = 0,1,\ldots,N \tag{34}$$

where s is the order of differentiation and $\mathrm{D} = \frac{2}{L}\mathrm{D}$ with D being the Chebyshev spectral differentiation matrix. Substituting Equations 31 to 34 in Equation 17 to 20 leads to the following linear matrix equation;

$$\mathrm{A}_{i-1}\mathrm{X}_i = \mathrm{R}_{i-1}, \tag{35}$$

subject to the boundary conditions;

$$f_i(\xi_k) = 0, \ \sum_{k=0}^{N} \mathrm{D}_{Nk} f_i(\xi_k) = 0, \quad \sum_{k=0}^{N} \mathrm{D}_{0k} f_i(\xi_k) = 0, \tag{36}$$

$$\theta_i(\xi_N) = \theta_i(\xi_0) = \phi_i(\xi_N) = \phi_i(\xi_0) = 0. \tag{37}$$

In Equation 35, A_{i-1} is a $(3N+3)\times(3N+3)$ square matrix, and X_i, R_{i-1} are $(3N+1)\times 1$ column vectors defined by the following equation;

$$\mathrm{A}_{i-1} = \begin{bmatrix} A_{11} & A_{12} & A_{13} \\ A_{21} & A_{22} & A_{23} \\ A_{31} & A_{32} & A_{33} \end{bmatrix}, \ \mathrm{X}_i = \begin{bmatrix} \mathrm{F}_i \\ \Theta_i \\ \Phi_i \end{bmatrix}, \ \mathrm{R}_{i-1} = \begin{bmatrix} \mathrm{r}_{1,i-1} \\ \mathrm{r}_{2,i-1} \\ \mathrm{r}_{3,i-1} \end{bmatrix}, \tag{38}$$

where

$$\mathrm{F}_i = [f_i(\xi_0), f_i(\xi_1), \ldots, f_i(\xi_{N-1}), f_i(\xi_N)]^T,$$

$$\Theta_i = [\theta_i(\xi_0), \theta_i(\xi_1), \ldots, \theta_i(\xi_{N-1}), \theta_i(\xi_N)]^T,$$

$$\Phi_i = [\phi_i(\xi_0), \phi_i(\xi_1), \ldots, \phi_i(\xi_{N-1}), \phi_i(\xi_N)]^T,$$

$$\mathrm{r}_{1,i-1} = [r_{1,i-1}(\xi_0), r_{1,i-1}(\xi_1), \ldots, r_{1,i-1}(\xi_{N-1}), r_{1,i-1}(\xi_N)]^T,$$

$$\mathrm{r}_{2,i-1} = [r_{2,i-1}(\xi_0), r_{2,i-1}(\xi_1), \ldots, r_{2,i-1}(\xi_{N-1}), r_{2,i-1}(\xi_N)]^T,$$

$$\mathrm{r}_{3,i-1} = [r_{3,i-1}(\xi_0), r_{3,i-1}(\xi_1), \ldots, r_{3,i-1}(\xi_{N-1}), r_{3,i-1}(\xi_N)]^T,$$

$$A_{11} = \mathrm{D}^3 + \mathrm{a}_{1,i-1}\mathrm{D}^2 - \frac{1}{\mathrm{Re}_D} + \mathrm{a}_{2,i-1}, \ A_{12} = \lambda \mathrm{I}, \ A_{13} = \lambda N_1 \mathrm{I},$$

$$A_{21} = \mathrm{b}_{2,i-1}, \ A_{22} = \mathrm{D}^2 + \mathrm{b}_{1,i-1}\mathrm{D}, \ A_{23} = D_f \mathrm{D},$$

where L is the scaling parameter used to invoke the boundary condition at infinity. The unknown functions f_i, θ_i and ϕ_i are approximated at the collocation points by the following equation;

$$A_{31} = \mathrm{c}_{2,i-1}, \ A_{32} = S_r \mathrm{D}^2, \ A_{33} = \mathrm{D}^2 + \mathrm{c}_{1,i-1}\mathrm{D}.$$

In the aforementioned definitions, $\mathrm{a}_{k,i-1}$, $\mathrm{b}_{k,i-1}$, and $\mathrm{c}_{k,i-1}$ $(k = 1,2)$ are diagonal matrices of size $(N+1)\times(N+1)$ and I is an identity matrix of size $(N+1)\times(N+1)$. After modifying the matrix system of Equation 35 to incorporate boundary conditions of Equations 36 to 37, the solution is obtained as the following equation;

$$\mathrm{X}_i = \mathrm{A}_{i-1}^{-1}\mathrm{R}_{i-1}. \tag{39}$$

To show the accuracy and robustness of the linearization method, Equations 12 to 14 were further solved numerically using the Keller-box implicit method described in the review paper (Keller, 1978). The Keller-box method gives second order accuracy and is unconditionally stable. Using this method the equations are first reduced to a system of first order equations, the resulting central difference equations linearized and then solved using the block-tridiagonal-elimination technique.

RESULTS AND DISCUSSION

In order to have a sense of the accuracy and reliability of the linearization technique, benchmark results were obtained for g_c and Re_D large. Table 1 gives a comparison between the results obtained using the linearization method and the numerical results based on the Chebyshev collocation method in Parand et al. (2010) as well as the homotopy analysis method (Liao,1999). It is evident that the linearization technique gives very accurate results when compared with the other two methods. Unless otherwise stated, the results in this study were obtained for $\mathrm{Pr} = 0.7$, $k_0 = 1$ and $\mathrm{Re}_D = 700$.

Tables 2 to 4 further give a sense of the accuracy and

Table 1. A comparison of values of $f''(0)$ obtained by the linearization method against (a) the Chebyshev collocation method of Parand et al. (2010) and, (b) the homotopy analysis method (HAM) solutions in Liao (1999) when $g_c = g_s = 0$, $\mathrm{Re}_D \to \infty$, $\mathrm{Pr} = 1$, $S_r = 0.3$, $D_f = 0.1$ and $Sc = 0.2$.

N	Parand et al. (2010)	Liao (1999)		Present method
	$f''(0)$	HAM order	$f''(0)$	$f''(0)$
	-	3	-	0.33205878
	-	4	-	0.33205733
6	0.33210951	5	0.28098	0.33205733
7	0.33210735	10	0.32992	0.33205733
8	0.33219404	15	0.33164	0.33205733
9	0.33206974	20	0.33198	0.33205733

Table 2. Effect of the temperature buoyancy parameter g_s on skin-friction, heat and mass transfer coefficients when $g_c = 0.1$, $S_r = 0.3$, $D_f = 0.1$ and $Sc = 0.2$.

	g_s	SLM order				Bvp4c solution	Keller box
		2nd	3rd	4th	5th		
$f''(0)$	0.1	0.653361	0.653355	0.653355	0.653355	0.653360	0.653363
	0.4	0.978436	0.978111	0.978111	0.978111	0.978095	0.978122
	0.8	1.358986	1.356569	1.356569	1.356569	1.356526	1.356581
Nu_x/Re_x	0.1	0.337183	0.337179	0.337179	0.337179	0.337182	0.337182
	0.4	0.369061	0.369073	0.369073	0.369073	0.369085	0.369077
	0.8	0.399966	0.399857	0.399857	0.399857	0.399864	0.399860
Sh_x/Re_x	0.1	0.151676	0.151676	0.151676	0.151676	0.151685	0.151676
	0.4	0.158695	0.158668	0.158668	0.158668	0.158675	0.158667
	0.8	0.165702	0.165478	0.165478	0.165478	0.165481	0.165475

Table 3. Effect of the Soret parameter on the skin-friction, heat and mass transfer coefficients when $g_c = g_s = 0.1$, $D_f = 0.1$, and $Sc = 0.2$.

	S_r	SLM order				Bvp4c solution	Keller box
		2nd	3rd	4th	5th		
$f''(0)$	0.0	0.637449	0.637446	0.637446	0.637446	0.637450	0.637453
	0.3	0.653361	0.653355	0.653355	0.653355	0.653360	0.653363
	0.6	0.669375	0.669362	0.669362	0.669362	0.669368	0.669370
Nu_x/Re_x	0.0	0.330915	0.330911	0.330911	0.330911	0.330915	0.330915
	0.3	0.337183	0.337179	0.337179	0.337179	0.337182	0.337182
	0.6	0.343594	0.343588	0.343588	0.343588	0.343591	0.343592
Sh_x/Re_x	0.0	0.205218	0.205218	0.205218	0.205218	0.205228	0.205218
	0.3	0.151676	0.151676	0.151676	0.151676	0.151685	0.151676
	0.6	0.095151	0.095153	0.095153	0.095153	0.095158	0.095151

Table 4. Effect of the Dufour parameter on the skin-friction, heat and mass transfer coefficients when $g_c = g_s = 0.1$, $Sr = 0.3$, and $Sc = 0.2$.

	D_f	SLM order				Bvp4c solution	Keller box
		2nd	3rd	4th	5th		
$f''(0)$	0.0	0.652489	0.652483	0.652483	0.652483	0.652489	0.652491
	0.4	0.656017	0.656010	0.656010	0.656010	0.656015	0.656018
	1.6	0.667364	0.667352	0.667352	0.667352	0.667358	0.667360
Nu_x/Re_x	0.0	0.339100	0.339095	0.339095	0.339095	0.339099	0.339099
	0.4	0.331218	0.331213	0.331213	0.331213	0.331216	0.331217
	1.6	0.303220	0.303212	0.303212	0.303212	0.303210	0.303217
Sh_x/Re_x	0.0	0.151200	0.151201	0.151201	0.151201	0.151209	0.151200
	0.4	0.153153	0.153153	0.153153	0.153153	0.153162	0.153153
	1.6	0.160041	0.160042	0.160042	0.160042	0.160050	0.160041

the rate of convergence of the linearization method when compared with the numerical results. Here we also demonstrate the effect of the physical parameters on the skin friction coefficient, Nusselt number and the Sherwood number. For all values of the physical parameters used, convergence of the method to the numerical results is achieved at the fifth order of the SLM approximation.

Table 2 shows the effect of increasing the temperature buoyancy on the skin-friction coefficient, Nusselt number and the Sherwood number. In practice it has been shown (Chang, 2006) that buoyancy effects are significant in forced convection when either the fluid velocity is relatively low or when the temperature difference between the wall and the free stream is large. Increases in the temperature buoyancy leads to an increase in the skin-friction coefficient, Nusselt number and the Sherwood number. The results earlier mentioned are similar to the recent findings (Singh et al., 2010) and are attributed to the fact that as the buoyancy increases, the fluid velocity inside boundary layer increases causing an increase in local skin-friction coefficient. The increased fluid velocity near the plate surface increases the heat transfer rate. Consequently, the drag exerted by the fluid on the plate is enhanced by increases in g_s.

Tables 3 and 4 show the effects of the Soret and Dufour parameters on the skin-friction coefficient, Nusselt number and the Sherwood number, it is evident that increasing Sr and Df leads to increasing skin friction coefficient. The increasing values of Sr results in increasing Nusselt number but decreasing the Sherwood number. However, the effect of Dufour parameter on heat and mass transfer is the exact opposite of the effect of Soret parameter as can be seen from Table 4.

To determine the influence of the physical parameters on the velocity, temperature and concentration profiles for the flow, we plot several curves of the velocity, temperature and concentration fields for different parameter values in Figures 1 to 9. The circles represent the linearization solution while the solid lines represent the numerical solution.

Figures 1 and 2 show the effect of increasing the temperature buoyancy parameters g_s on the velocity, temperature and concentration profiles. We note here (Alam et al., 2006) that the dimensionless parameter g_c has the same meaning and effect as g_s. The buoyancy is assumed to be such that $g_s \leq 1$ representing pure forced convection ($g_s << 1$) and mixed convection ($g_s = 1$). For pure forced convection, increasing the buoyancy leads to steady increases in the velocity. Figure 2 shows that increasing the buoyancy leads to decreases in the temperature $\theta(\eta)$ and in the concentration $\phi(\eta)$ profiles. The results are line with other studies in the literature (Alam et al., 2006).

The effects of increasing the Schmidt number Sc on the velocity, temperature and the concentration profiles are shown in Figures 3 and 4. The velocity and the concentration decrease with increasing Sc, increasing Sc leads to increases on temperature profile. The Schmidt number Sc characterizes a fluid flow in which there is simultaneous momentum and mass diffusion convection processes. The effects of Soret parameter on the velocity, temperature and the concentration have been shown in Figures 6 and 7. The velocity and the concentration profiles increase with increasing S_r whereas the temperature decreases lightly with increases in S_r.

Figures 8 and 9 show the effects of the Dufour parameter on the fluid properties. The velocity and the temperature increase when D_f increases. However

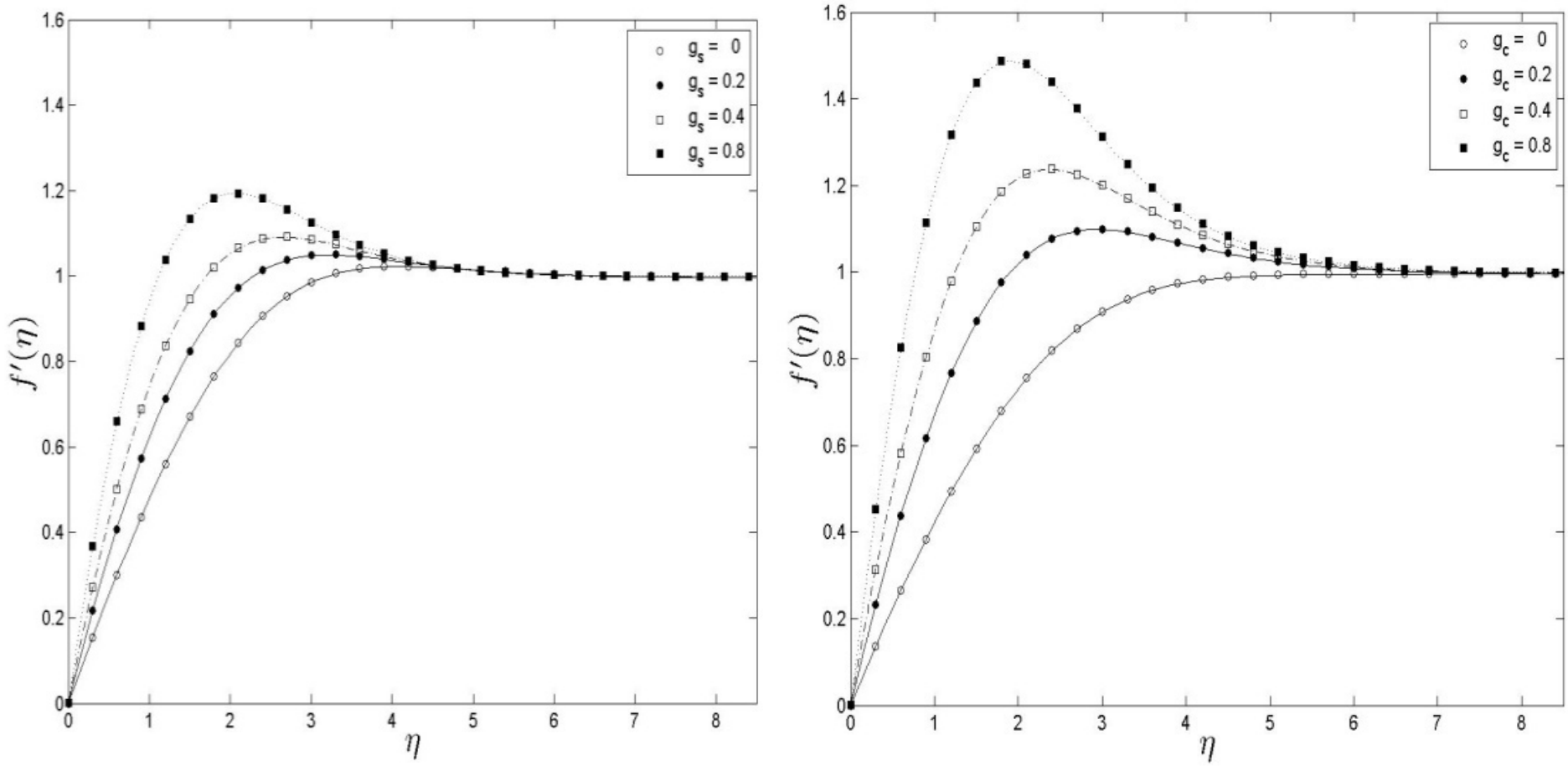

Figure 1. Effect of the temperature and concentration buoyancy parameters g_c and g_s on the velocity profiles when $S_r = 0.3$, $D_f = 0.1$ and $Sc = 0.2$.

increasing D_f leads to decreases in the concentration profile.

Conclusion

In this paper we investigated the free convection flow with cross-diffusion and double diffusive using a novel successive linearization (SLM) method. Comparison between the solutions obtained using the linearization method, the Keller-box implicit method and the Matlab bvp4c numerical routine has been shown in Tables 1 to 3. The convergence of the method is rapid. The influence of the governing parameters on the fluid properties has also been shown graphically. Increasing the buoyancy leads to increases in the velocity, but decreases the temperature and the concentration. The effect of the Soret parameter is to increase the velocity and the concentration, and to decrease the temperature profiles. The Dufour parameter increases the velocity and the

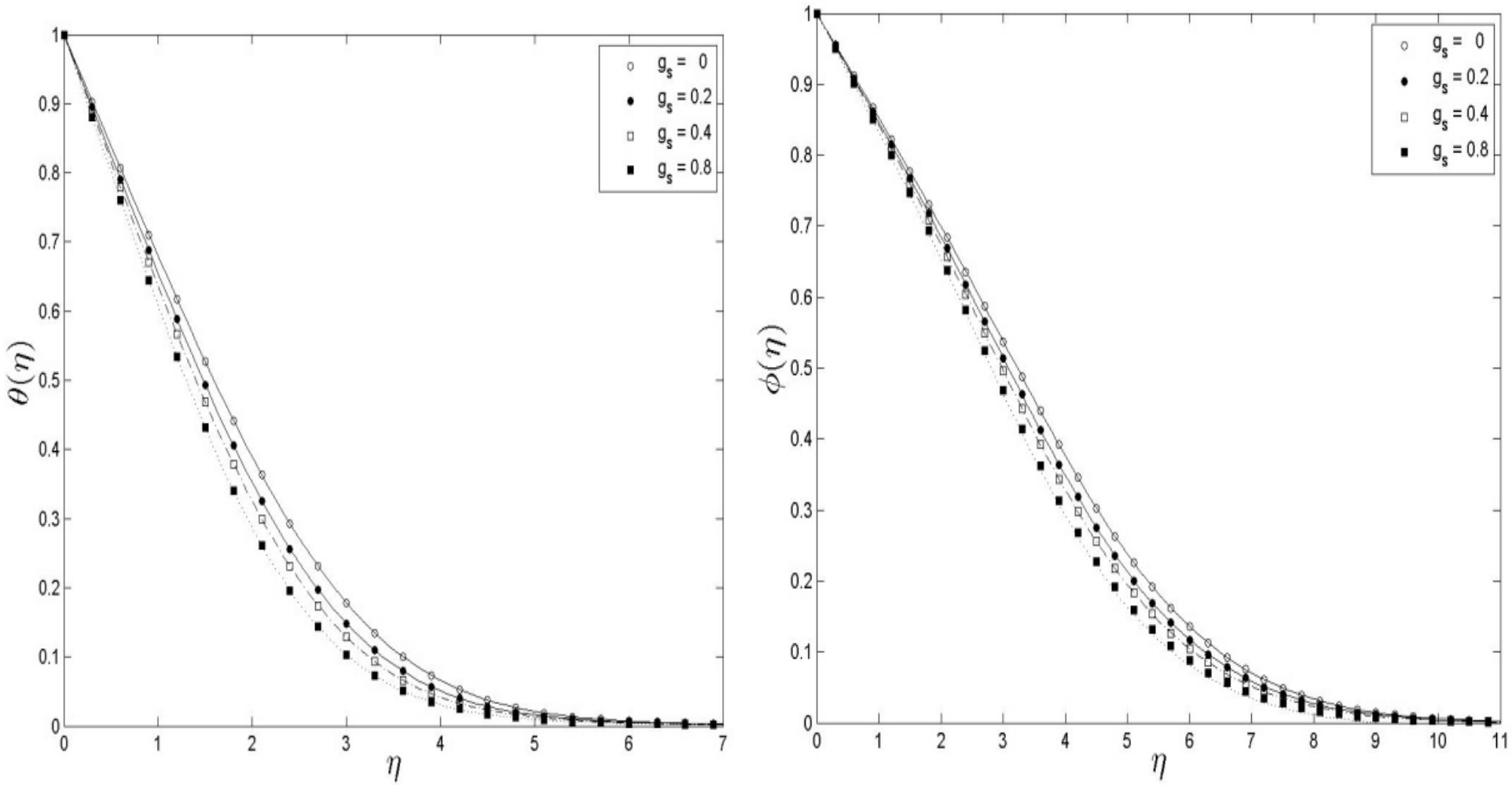

Figure 2. Effect of the temperature buoyancy parameter g_s on the temperature and concentration profiles when $g_c = 0.1$, $S_r = 0.3$ and $D_f = 0.1$.

temperature but has only a slight effect on the concentration profiles. The velocity increases by increasing the buoyancy parameter. The temperature as well as concentration however decrease with an increase in the buoyancy parameter. The velocity and the concentration decrease with increasing Schmidt numbers. The temperature however increase with increases in Schmidt numbers.

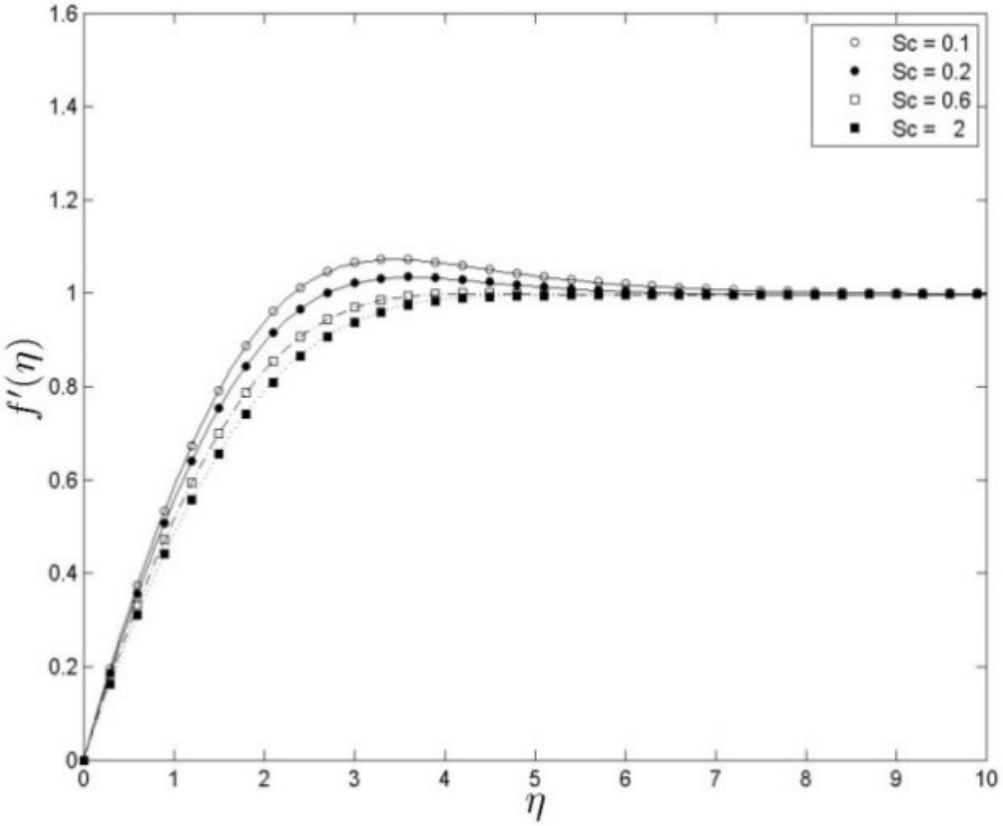

Figure 3. Variation of the velocity profile with the Schmidt number Sc when $g_c = g_s = 0.1$, $S_r = 0.3$, and $D_f = 0.1$.

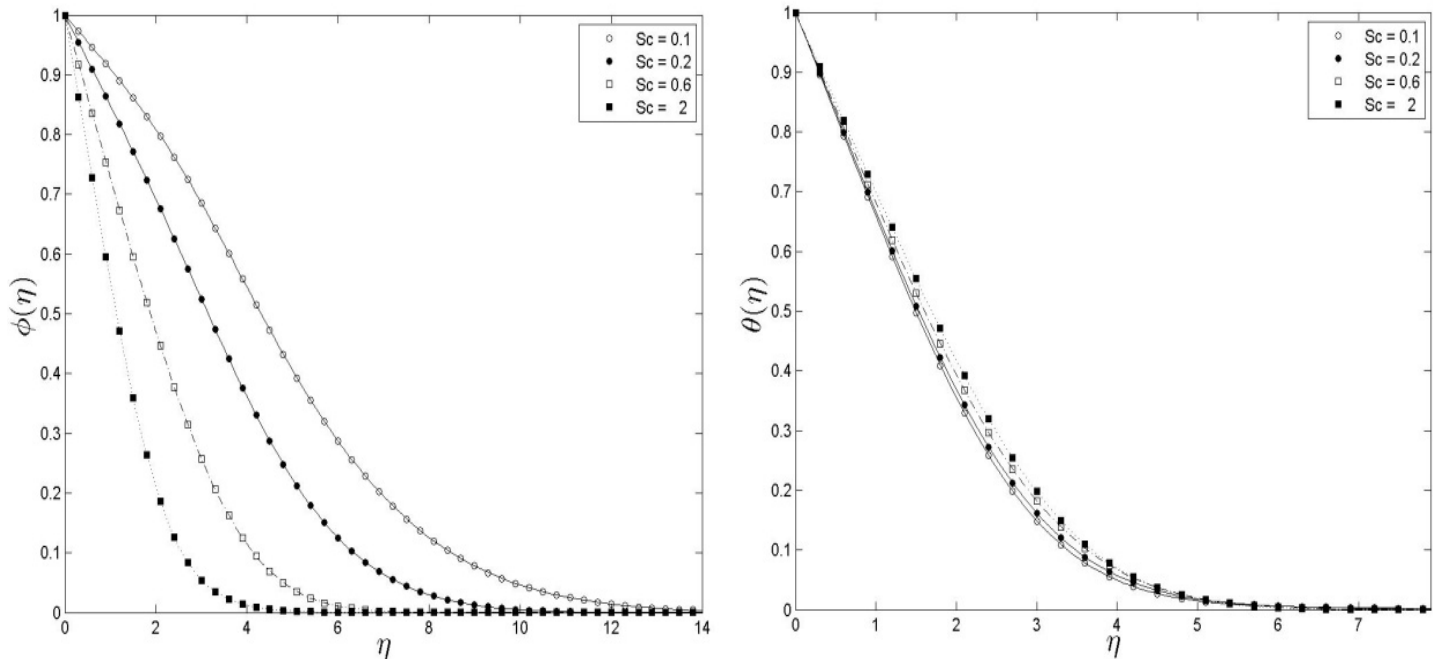

Figure 4. Variation of the temperature and concentration curves with Sc when $g_c = g_s = 0.1$, $S_r = 0.3$, and $D_f = 0.1$.

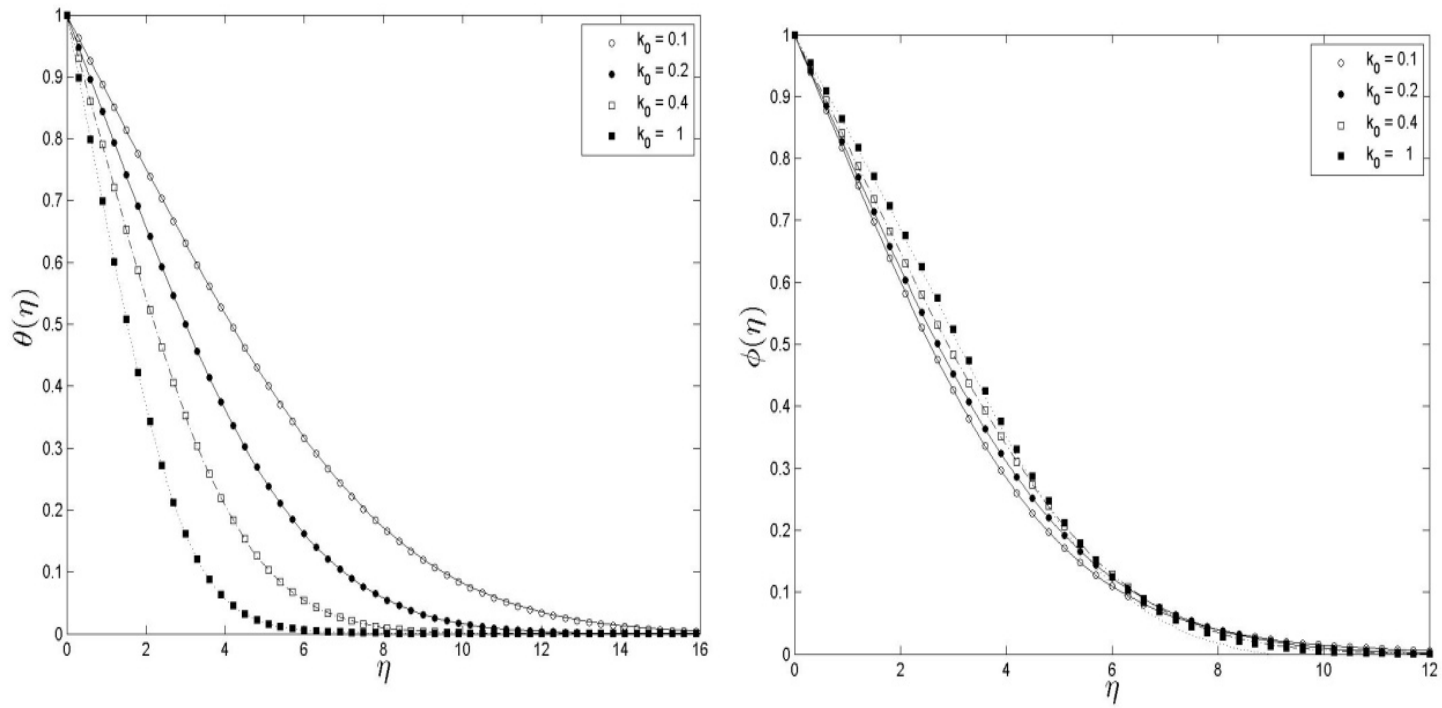

Figure 5. Variation of the temperature and concentration curves with k_0 when $g_c = g_s = 0.1$, $S_r = 0.3$, $D_f = 0.1$ and $Sc = 0.2$.

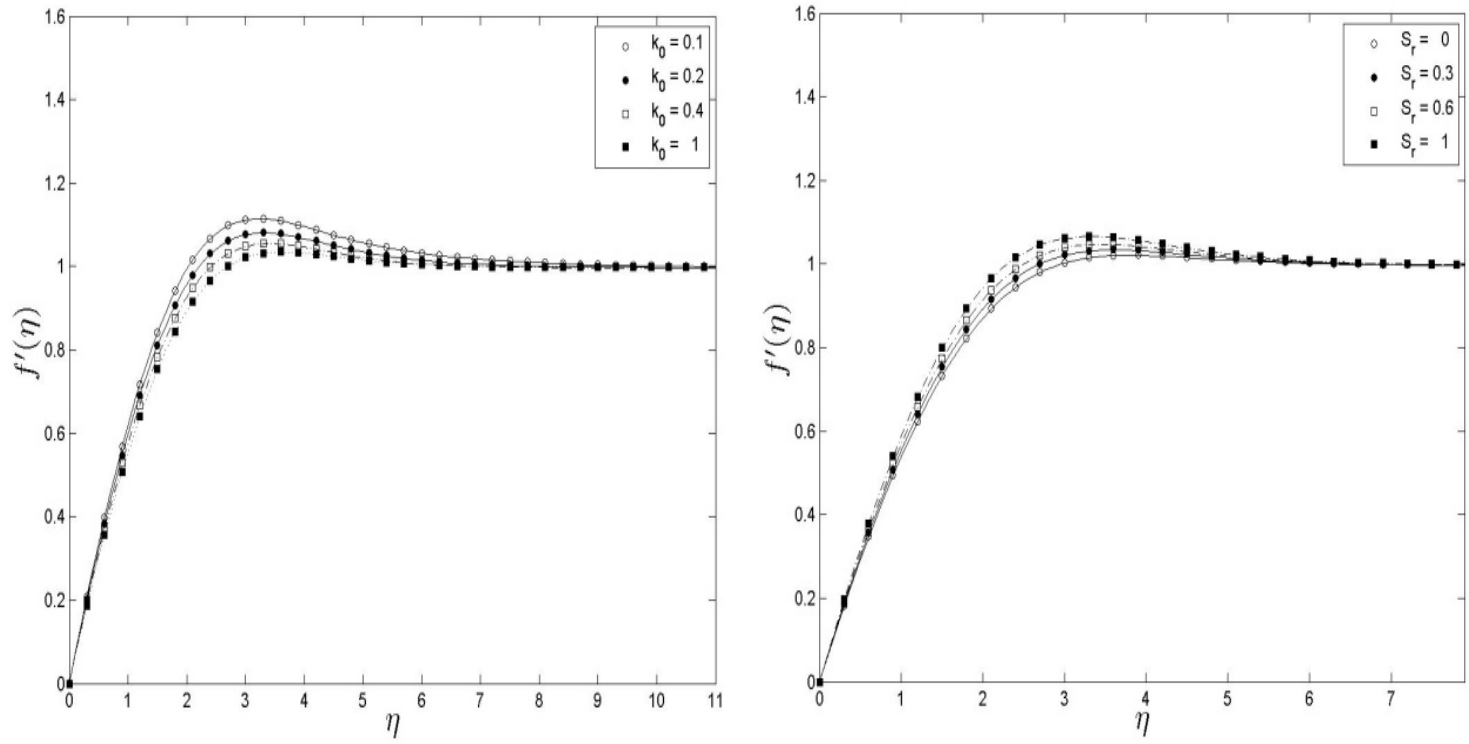

Figure 6. Variation of the velocity profile with (a) k_0 ($S_r = 0.3$), and (b) S_r when $k_0 = 1$. The other parameters are $g_c = g_s = 0.1$, $Sc = 0.2$ and $D_f = 0.1$.

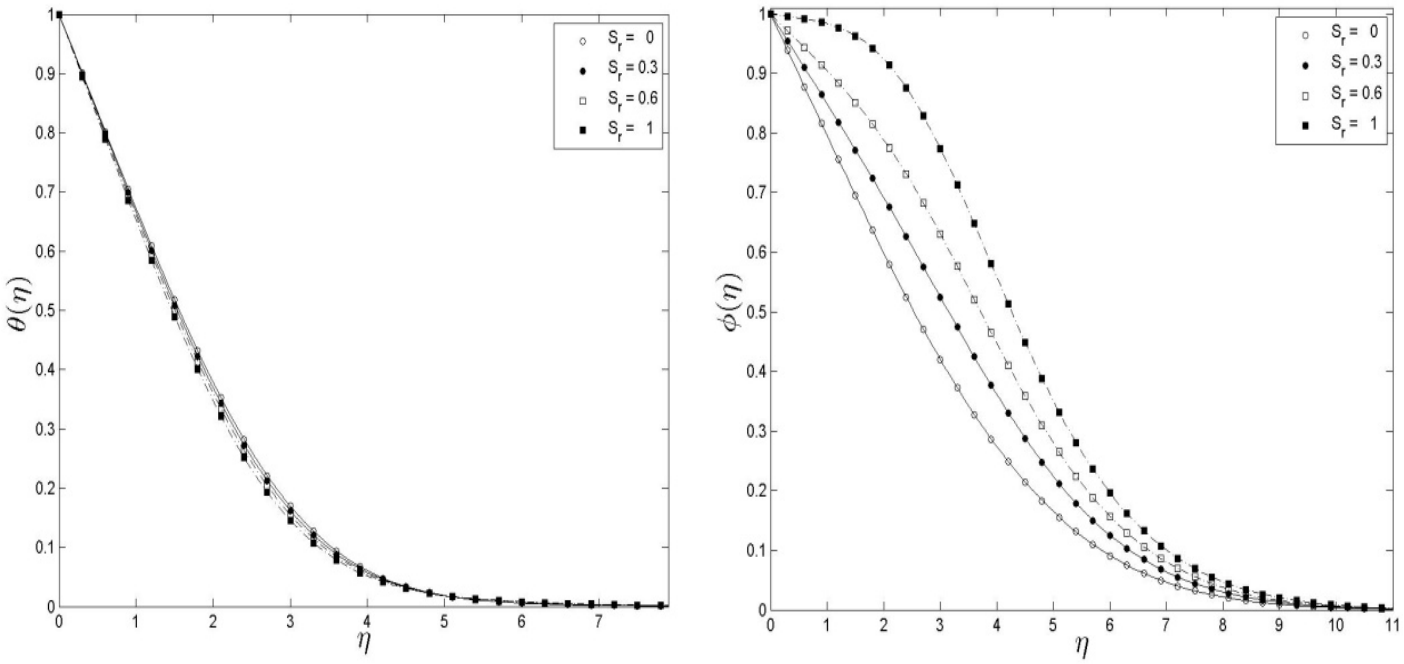

Figure 7. Variation of the temperature and concentration curves with S_r when $g_c = g_s = 0.1$, $D_f = 0.1$ and Sc = 0.2 and $Sc = 0.2$.

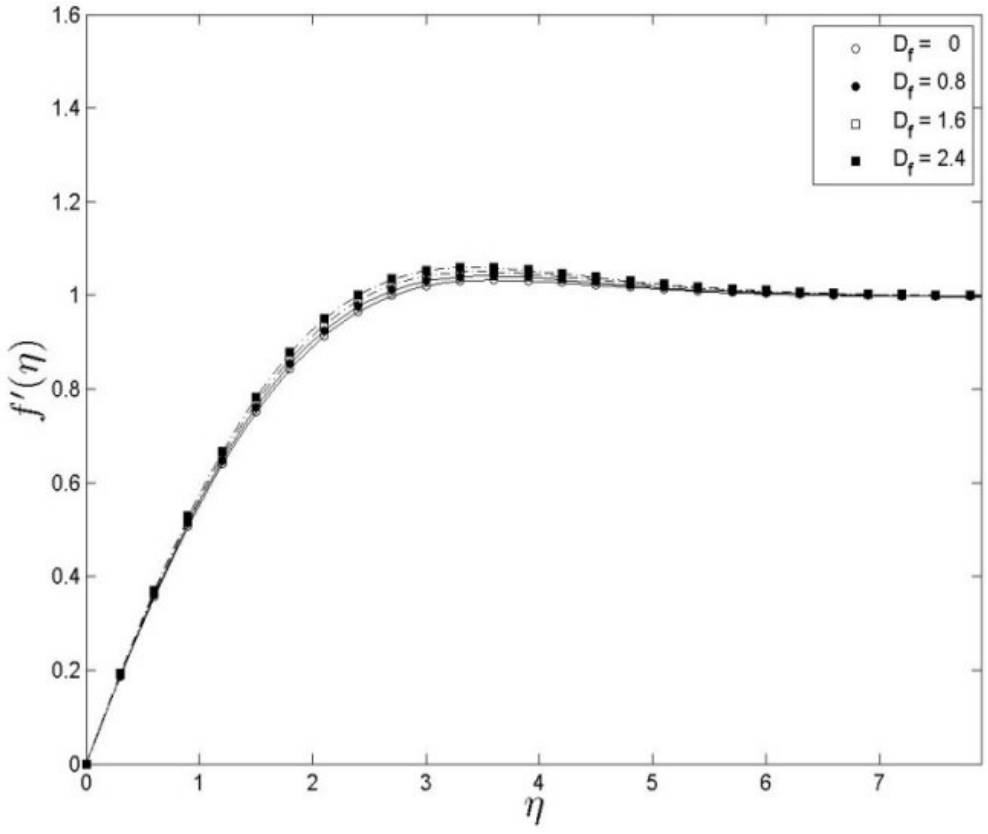

Figure 8. Variation of the velocity profile with D_f when $g_c = g_s = 0.1$, $S_r = 0.3$ and $Sc = 0.2$.

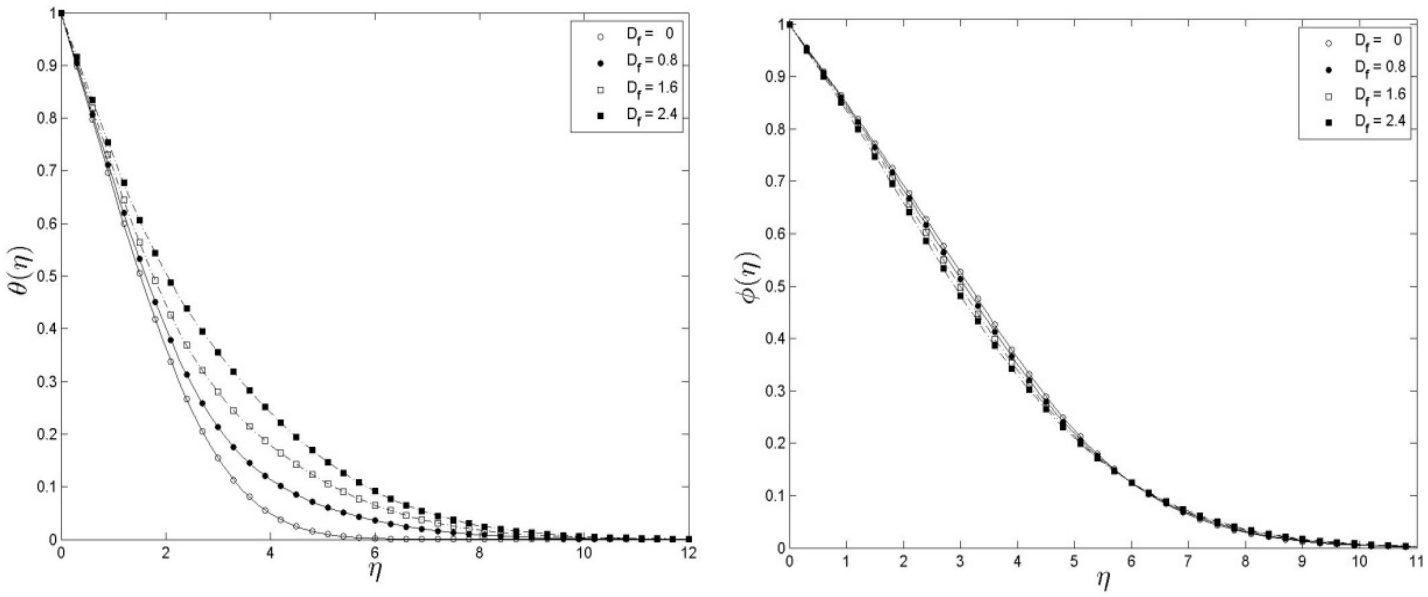

Figure 9. Variation of the temperature and concentration curves with S_r when $g_c = g_s = 0.1$, $D_f = 0.1$ and $Sc = 0.2$.

REFERENCES

Abreu CRA, Alfradique MF, Silva Telles A (2006). Boundary layer flows with Dufour and Soret effects: Forced and natural convection. Chem. Eng. Sci., 61:4282- 4289.

Alam MS, Rahman MM, Samad MA (2006). Dufour and Soret effects on unsteady MHD free convection and mass transfer flow past a vertical porous plate in a porous medium. Nonlinear Analysis. Model. Control, 11:217-226.

Anghel M, Takhar HS, Pop I (2000). Dufour and Soret effects on free convection boundary-layer over a vertical surface embedded in a porous medium. Studia Universitatis Babes-Bolyai Mathematica, XLV(4):11- 21.

Atimtay AT, Gill WN (1985). The effect of free stream concentration on heat and binary mass transfer with thermodynamic coupling in convection on a rotating disc. Chem. Eng. Commun. 34:161- 185.

Awad FG, Sibanda P, Motsa SS (2010). On the linear stability analysis of a Maxwell fluid with double-diffusive convection. Appl. Math. Model., 34:3509 - 3517.

Awad FG, Sibanda P, Motsa SS, Makinde OD (2011). Convection from an inverted cone in a porous medium with cross-diffusion effects. Comput. Math. Appl., 61:1431-1441.

Bejan A, Khair KR (1985). Heat and mass transfer by natural convection in a porous medium. Int. J. Heat Mass Transf., 28:909- 918.

Chang CL (2006). Buoyancy and wall conduction effects on forced convection of micropolar fluid flow along a vertical slender hollow circular cylinder. Int. J. Heat Mass Transf., 49:4932- 4942.

Cheng CY (2009). Soret and Dufour effects on natural convection heat and mass transfer from a vertical cone in a porous medium. Int. Commun. Heat Mass Transf., 36:1020 - 1024.

Eckert ERG, Drake RM (1972). Analysis of Heat and Mass Transfer. McGraw-Hill, New York.

El-Aziz MA (2009). Radiation effect on the flow and heat transfer over an unsteady stretching sheet. Int. Commun. Heat Mass Transf., 36:521-524.

Erickson LE, Fan LT, Fox VG (1966). Heat and mass transfer on a moving continuous flat plate with suction or injection. Ind. Eng. Chem. Fundam., 5:19 - 25.

Fox VG, Erickson LE, Fan LT (1968). Methods for solving the boundary layer equations for moving continuous flat surfaces with suction and injection. AIChE J. 14:726 – 736.

Gupta PS, Gupta AS (1977). Heat and mass transfer with suction and blowing. Can. J. Chem. Eng. 55:744 – 746.

Hossain MA, Takhar HS (1996). Radiation effect on mixed convection along a vertical plate with uniform surface temperature. Heat Mass Transf., 31:243-248.

Keller HB (1978). Numerical methods in boundary-layer theory. Ann. Rev. Fluid Mech., 10:417- 433.

Liao SJ (1999). An explicit, totally analytic approximate solution for Blasius viscous flow problem. Int. J. Nonlinear Mech., 34:759- 778.

Mahdy A (2010). Soret and Dufour effect on double diffusion mixed convection from a vertical surface in a porous medium saturated with a non-Newtonian fluid. J. Non-Newtonian Fluid Mech., 165:568 - 575.

Makinde OD (2011). MHD mixed-convection interaction with thermal radiation and nth order chemical reaction past a vertical porous plate embedded in a porous medium. Chem. Eng. Commun., 198(4): 590-608.

Makinde OD, Aziz A (2010). MHD mixed convection from a vertical plate embedded in a porous medium with a convective boundary condition. Int. J. Thermal Sci., 49: 1813-1820.

Makinde OD, Sibanda P. (2008). Magnetohydrodynamic mixed convective flow and heat and mass transfer past a vertical plate in a porous medium with constant wall suction. ASME – J. Heat Transfer, 130:112602.

Makinde OD, Ogulu A (2008). The effect of thermal radiation on the heat and mass transfer flow of a variable viscosity fluid past a vertical porous plate permeated by a transverse magnetic field. Chem. Eng. Commun, 195(12): 1575 -1584.

Malashetty MS, Gaikad SN (2002). Effect of cross diffusion on double diffusive convection in the presence of horizontal gradients. Int. J. Eng. Sci., 40: 773 - 787.

Mortimer RG, Eyringt H (1980). Elementary transition state theory of the Soret and Dufour effects. Proc. National Acad. Sci. 77: 1728 - 1731.

Motsa SS, Sibanda P, Shateyi S (2011). On a new quasi-linearization method for systems of nonlinear boundary value problems. Math. Meth. Appl. Sci. 34:1406-1413.

Narayana PAL, Sibanda P (2010). Soret and Dufour effects on free convection along a vertical wavy surface in a fluid saturated Darcy porous medium. Int. J. Heat Mass Transf., 53:3030 - 3034.

Parand K, Shanini M, Dehghan M (2010). Solution of a laminar boundary layer flow via a numerical method. Commun Nonlinear Sci Numer Simulat. 5:360 - 367.

Partha MK (2009). Suction/injection effects on thermophoresis particle deposition in a non-Darcy porous medium under the influence of Soret, Dufour effects. Int. J. Heat Mass Transf., 52:1971 - 1979.
Postelnicu A (2004). Influence of a magnetic field on heat and mass transfer by natural convection from vertical surfaces in porous media considering Soret and Dufour effects. Int. J. Heat Mass Transf., 47:1467 - 1472.
Raptis A, Perdikis C (1998). Viscoelastic flow by the presence of radiation. ZAMM. 78:277 - 279.
Rapits A (1998). Flow of a micropolar fluid past a continuously moving plate by the presence of radiation. Int. J. Heat Mass Transf., 41:2865 - 2866.
Reddy MG, Reddy NB (2010). Soret and Dufour effects on steady MHD free convection flow past a semi-infinite moving vertical plate in a porous medium with viscous dissipation. Int. J. Appl. Math. Mech., 6:1-12.
Rosner DE (1980). Thermal (Soret) diffusion effects on interfacial mass transport rates. Physicochem. Hydrodyn., 1:159 - 185.
Shateyi S, Motsa SS, Sibanda (2010). The effects of thermal radiation, Hall currents, Soret, and Dufour on MHD flow by mixed convection over a vertical surface in porous media. Mathematical Problems in Engineering. Article ID 627475, 20 pages doi:10.1155/2010/627475.
Shateyi S, Motsa SS (2009). Thermal radiation effects on heat and mass transfer over an unsteady stretching surface. Mathematical Problems in Engineering. Article ID 965603, 13 pages doi:10.1155/2009/965603.
Singh G, Sharma PR, Chamkha AJ (2010). Effect of thermally stratified ambient fluid on MHD convective flow along a moving non-isothermal vertical plate. Int. J. Phys. Sci. 5: 208 - 215.
Tsai R, Huang JS (2009). Heat and mass transfer for Soret and Dufour's effects on Hiemenz flow through porous medium onto a stretching surface. Int. J. Heat Mass Transf., 52:2399 - 2406.
Weaver JA, Viskanta R (1991). Natural convection due to horizontal temperature and concentration gradients II. Species interdiffusion, Soret and Dufour effects. Int. J. Heat Mass Transf., 34:3121- 3133.
Yu X, Guo Z, Shi B (2007). Numerical study of cross-diffusion effects on double diffusive convection with lattice Boltzmann method. In: Y Shi et al. (Eds): ICCS, LNCS 4487:810 - 817.